Asymmetric Frequency Conversion in Nonlinear Systems Driven by a Biharmonic Pump

Archana Kamal,[1,2,*] Ananda Roy,[1] John Clarke,[3] and Michel H. Devoret[1]

[1]*Departments of Physics and Applied Physics, Yale University, New Haven, Connecticut 06520, USA*
[2]*Research Laboratory of Electronics, Massachusetts Institute of Technology, Cambridge, Massachusetts 02139, USA*
[3]*Department of Physics, University of California, Berkeley, California 94720-7300, USA*

A novel mechanism of asymmetric frequency conversion is investigated in nonlinear dispersive devices driven parametrically with a biharmonic pump. When the relative phase between the first and second harmonics combined in a two-tone pump is appropriately tuned, nonreciprocal frequency conversion, either upward or downward, can occur. Full directionality and efficiency of the conversion process is possible, provided that the distribution of pump power over the harmonics is set correctly. While this asymmetric conversion effect is generic, we describe its practical realization in a model system consisting of a current-biased, resistively shunted Josephson junction. Here, the multiharmonic Josephson oscillations, generated internally from the static current bias, provide the pump drive.

PACS numbers: 85.25.Cp, 42.65.Ky

Directed transport in nonlinear systems driven by a signal that breaks time-reversal symmetry has received much attention in the last decade [1–5]. This class of systems is closely connected to that of driven systems in which a degree of freedom moves in a potential lacking space inversion symmetry [6]. These various subjects address what is popularly known as the "ratchet effect" [7]. Here, we focus our attention on a particular type of transport, namely, frequency conversion of a signal with the carrier being translated in frequency space either upward (up-conversion process) or downward (down-conversion process). While familiar devices with a purely dispersive nonlinearity, such as 3-wave or 4-wave mixers, can readily perform frequency conversion, reciprocity is maintained between up- and down-converted photon amplitudes with the two directions being distinguished solely by a relative phase determined by the pump tone [8].

In this Letter, we demonstrate that when the drive contains both the first and second harmonics, either up- or down-conversion can be selected provided the relative phase and amplitude of the tones are set appropriately. Moreover, since this asymmetric conversion process can operate without dissipation in a dispersive nonlinear element such as a superconducting Josephson junction, it can be extended to the quantum regime where signals consist of coherently superposed photon states. Furthermore, a detailed understanding of the conditions under which asymmetric conversion can take place will be useful in the design of quantum information processing protocols in mesoscopic devices. As an example, we show that asymmetric frequency conversion takes place in the current-biased, resistively shunted Josephson junction (RSJ).

To begin with a general discussion, we consider a generic nonlinear system consisting of two parametrically coupled oscillators *A* and *B*. We model the parametric coupling as a time-varying mutual inductance $M(t)$, as shown in Fig. 1(a). Varying this coupling at the pump frequency ω_p at the difference or sum of the two coupled modes results in three-wave mixing, leading to either frequency conversion or amplification, respectively [9]. In microwave circuits such a coupling scheme may be implemented
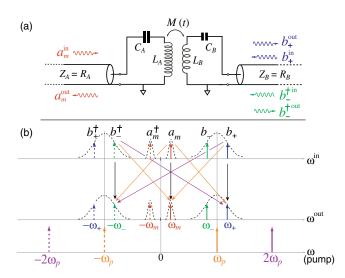

FIG. 1 (color online). Asymmetric parametric frequency converter. (a) Minimal model based on a time-varying mutual inductance $M(t)$ with frequencies ω_p and $2\omega_p$. (b) Frequency landscape showing various frequency mixing processes between the modulation frequency ω_m and the sidebands at $\omega_\pm$; solid and dashed arrows indicate the amplitudes of different modes and their conjugates, respectively. The modulation frequency ω_m is chosen to coincide with the center resonance ω_A of the low frequency oscillator, and the pump tone ω_p is chosen to coincide with the center resonance ω_B of the high frequency oscillator. The colors of the mixing arrows indicate the colors of the relevant pump frequencies mediating the process, as shown on the separate pump axis. The black arrows indicate reflections.

by employing the nonlinear Josephson inductance, $L_J(I) = L_J(0)[1 - (I/I_0)^2]^{-1/2}$. When the current $I(t) = i_{rf}\cos(\omega_p t)$ flowing through the junction is much smaller than the critical current I_0, the junction behaves as an effective time-varying inductance $L_J(t) \approx L_J(0)I(t)/I_0$ modulated at the pump frequency by the rf current $I(t)$. In Fig. 1(b), we show a more generic configuration [10] where the pump frequency ω_p is aligned with the oscillator resonance ω_B, fulfilling the conversion condition $(\omega_P = \omega_+ - \omega_A)$ with respect to the upper sideband at ω_+ and the amplification condition $(\omega_P = \omega_- + \omega_A)$ with respect to the lower sideband at ω_-.

A convenient formalism to capture the dynamics of such parametric systems is provided by input-output theory [11]. In this paradigm, a three-wave mixer is fully described by a scattering matrix that gives the relationship between each incoming and outgoing mode of the system,

$$\begin{pmatrix} a^{\text{out}}[\omega_m] \\ b^{\text{out}}[\omega_+] \\ b^{\text{out}}[-\omega_-] \end{pmatrix} = \begin{pmatrix} r_m & t_d & s_d \\ t_u & r_+ & v_{+-} \\ s_u & v_{-+} & r_- \end{pmatrix} \begin{pmatrix} a^{\text{in}}[\omega_m] \\ b^{\text{in}}[\omega_+] \\ b^{\text{in}}[-\omega_-] \end{pmatrix}, \quad (1)$$

where different frequency components participating in the mixing process, ω_m and $\omega_\pm = \omega_p \pm \omega_m$, are selected by harmonic balance. The a and b denote incoming and outgoing wave amplitudes for spatial channels A and B, normalized in terms of single photon energies, such that $\langle a^{\text{in,out}}[\omega]a^{\text{in,out}}[\omega']\rangle = S_{a^{\text{in,out}}a^{\text{in,out}}}[(\omega - \omega')/2]\delta(\omega + \omega')$ where $S_{a^{\text{in,out}}a^{\text{in,out}}}[\omega]$ represents the number of photons per unit time per unit bandwidth around frequency ω. Negative frequency amplitudes denote conjugation along with conversion; for real signals $a[-\omega] = a^\dagger[\omega]$. Here t_u, s_u describe up-conversion from the modulation frequency ω_m to sideband frequencies $\pm\omega_p + \omega_m$ while t_d, s_d describe the reverse process of down-conversion from sideband frequencies to the modulation frequency. The diagonal elements denoted by $r_{m,+,-}$ are the respective reflection coefficients, and the $v_{\pm\mp}$ coefficients denote the strength of mixing within the sidebands. The frequency landscape in Fig. 1(b) depicts these processes pictorially. All the three-wave mixing processes considered here are assumed to be phase matched since the mixing process is spatially local in the lumped element geometry shown in Fig. 1. Hence, the phases of the signals are entirely determined by the phase of the corresponding pump mediating the mixing process. In addition, the oscillation amplitudes at signal and sideband frequencies are considered to be weak enough to be in the linear input-output regime, where instabilities and nonlinearities due to pump depletion [8,12] can be safely ignored.

We now consider two distinct pumping schemes.

Case I:—$M(t) = M_1\cos(\omega_p t)$. This corresponds to the usual case of parametric pumping with a monochromatic tone. Following an analysis similar to that in [10], we obtain

$$t_d = t_u = 2i\xi_1, \qquad (2a)$$

$$s_d = s_u^* = 2i\xi_1, \qquad (2b)$$

$$v_{+-} = 2\xi_1^2; \qquad v_{-+} = -2\xi_1^2, \qquad (2c)$$

where $\xi_1 = (M_1/\sqrt{L_A L_B})$ is the equivalent dimensionless pump strength [13]. Thus, we recover the usual case of symmetric (or reciprocal) frequency conversion with scattering between any pair of signals of equal magnitude, i.e. $|t_d| = |t_u|, |s_d| = |s_u|$. We note, however, that the phases associated with the off-diagonal scattering elements are not equal. For mathematical simplicity, we work under the rotating wave approximation (RWA) and assume that both oscillators A and B are driven near resonance, i.e. $\omega_m = \omega_A$ and $\delta_\pm = (\omega_\pm - \omega_B)/\Gamma_B \ll 1$ [$\Gamma_B = R_B/(2L_B)$ is the line width of the high frequency oscillator].

Case II:—$M(t) = M_1\cos(\omega_p t) + M_2\cos(2\omega_p t + \alpha)$. In the case of biharmonic driving, additional three-wave mixing of sidebands by the $2\omega_p$ harmonic modifies the scattering amplitudes to (assuming $\delta_\pm = 0$)

$$t_d = 2i\xi_1 D(1 + ie^{-i\alpha}\xi_2); \qquad t_u = 2i\xi_1 D(1 + ie^{i\alpha}\xi_2), \qquad (3a)$$

$$s_d = 2i\xi_1 D(1 - ie^{i\alpha}\xi_2); \qquad s_u = -2i\xi_1 D(1 - ie^{-i\alpha}\xi_2), \qquad (3b)$$

$$v_{+-} = 2D(\xi_1^2 + ie^{i\alpha}\xi_2); \qquad v_{-+} = -2D(\xi_1^2 + ie^{-i\alpha}\xi_2), \qquad (3c)$$

where $\xi_2 = (M_2/\sqrt{L_A L_B})$ and $D = [2i\xi_1^2\xi_2\cos\alpha + (1 - \xi_2^2)]^{-1}$. Equation (3) shows that the usual symmetry of frequency conversion is now broken, since $|t_d| \neq |t_u|$ and $|s_d| \neq |s_u|$. Moreover, the preferred conversion channel is guided by α, the phase shift between the harmonic components of the drive. Maximum asymmetry between off-diagonal scattering coefficients is obtained for $\alpha = \pm\pi/2$, with $+\pi/2$ yielding down-conversion and $-\pi/2$ yielding up-conversion (Fig. 2). For zero phase difference between the two harmonics, $\alpha = 0(\text{mod}2n\pi)$, we recover symmetric scattering, although with modified coefficients because of additional 3-wave mixing by the $2\omega_p$ pump. The physical mechanism underlying this asymmetry is rooted in the interference of different conversion paths in frequency space between a given pair of modes. As shown in Fig. 2(c), the phases of different scattering coefficients are governed by the phases of respective harmonics mediating the process. The introduction of three-wave mixing processes between the sidebands $\omega_\pm$ closes the interference loop; the phase sensitive nature of up- and down-conversion coefficients (t, s), obtained with the single-frequency pump in *case I*, is translated through these processes into an asymmetry between off-diagonal scattering amplitudes.
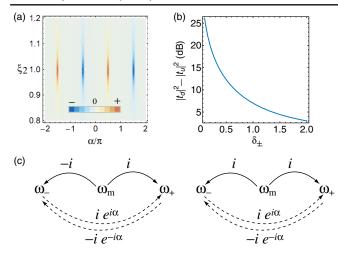
FIG. 2 (color online). Asymmetric frequency conversion. (a) Asymmetry between frequency conversion amplitudes $|t_d|^2 - |t_u|^2$ [Eq. (3)] plotted as a function of the strength of the second harmonic (ξ_2) of the pump and phase frustration α between the harmonics. Maximum asymmetry is realized for maximal frustration $\alpha = \pi/2 \pm n\pi$, with down-conversion occurring when the second harmonic leads the first harmonic ($\alpha = +\pi/2 + 2n\pi$) and up-conversion occurring when the second harmonic lags behind the first harmonic ($\alpha = -\pi/2 + 2n\pi$). (b) Maximal asymmetry plotted as a function of modulation frequency parametrized as dimensionless detuning $\delta_\pm = \omega_m/\Gamma_B$. (c) Interference of different scattering amplitudes showing the realization of asymmetry as in (a). Solid lines indicate the usual frequency conversion in the presence of a single monochromatic pump at frequency ω_p while the dashed arrows indicate additional processes mediated by its second harmonic $2\omega_p$.

Biharmonically pumped parametric systems form an intriguing platform for exploring qualitatively new physics, the asymmetric frequency conversion discussed here being one such example. Steady state properties near the critical bifurcation threshold in such systems have also been studied in detail previously [14], with photon statistics displaying bunching or antibunching depending on the relative phase between the two pump drives [15]. Furthermore, in conjunction with the recently proposed ideas of reservoir engineering [16], such parametric conversion protocols can be shown to implement quantum-limited directional amplification [17,18].

As an example of a multiharmonic-pump mediated frequency conversion, we now consider in detail the scattering of a microwave signal by an RSJ current biased in its voltage state. The RSJ has been studied extensively both theoretically [19,20] and experimentally [21,22]. The phenomenon of directed transport in a single-junction functioning as fluxon ratchets has also received attention [23,24], though these studies have focussed on the static current-voltage characteristics. On the other hand, studies of mixer properties of the RSJ have remained restricted to considering Josephson oscillations as the carrier or local oscillator [25]. Detailed studies of higher Josephson harmonics in the RSJ have remained elusive, to the best of our

knowledge, and the emergence of dynamical nonreciprocity under their influence has remained hitherto unexplored. Here, we present a generalized input-output formalism that enables a self-consistent analytical evaluation of amplitudes and phases of Josephson harmonics, generated internally by the ac Josephson effect, to any order.

We begin with the well-known nonlinear equation of motion for a Josephson junction biased with a static current I_B,

$$\frac{\varphi_0}{R}\dot{\varphi} + I_0 \frac{\partial}{\partial\varphi}\left(\frac{U}{E_J}\right) = 0, \qquad (4)$$

representing a particle moving in the washboard potential $U(\varphi) = E_J(1 - \cos\varphi - \varphi I_B/I_0)$. Here, φ denotes the phase difference across the junction, $E_J = \varphi_0 I_0$ is the Josephson energy, I_0 the critical current, $\varphi_0 = \hbar/(2e)$ the reduced flux quantum and R the shunt resistance. The presence of the $\cos\varphi$ term in $U(\varphi)$ causes the dynamics to be highly nonlinear, generating multiple Josephson harmonics for $I_B > I_0$. These harmonics play a role analogous to that of the multiharmonic pump discussed earlier. To describe the mixing properties of the RSJ, we perform a perturbative analysis by expressing the phase as $\varphi = \omega_J t + \delta\varphi(t)$ and expanding the $\cos\varphi$ term in a series in $\delta\varphi$ about $\omega_J t$, where $\omega_J = \langle\dot{\varphi}\rangle$ is the Josephson frequency.

This treatment allows us to write

$$\delta\varphi(t) = \sum_{k=1}^{K} p_k^I \cos(k\omega_J t) + p_k^Q \sin(k\omega_J t) \qquad (5)$$

in terms of the harmonic components associated with the junction dynamics. Here, (p_k^I, p_k^Q) denotes the amplitudes of the two quadratures associated with the kth harmonic of ω_J. Following the analysis scheme introduced earlier [26], we evaluate $p_k^{I,Q}$ for different k values as a truncated power series in the dimensionless inverse bias parameter $x = I_0/I_B$, with the number of Josephson harmonics K included in the calculation set by the order of expansion of $\cos\varphi$. A self-consistent calculation of the static $I - V$ characteristics, which are related to the amplitudes of the Josephson oscillation and its harmonics, is presented in Fig. 4(a).

The calculated amplitude of the Josephson oscillation using this method to first order [corresponding to $K = 1$ in Eq. (5)] is [27]

$$p_1^I = x; \qquad p_1^Q = 0.$$

Similarly, including the next order in the perturbation series [corresponding to $K = 2$ in Eq. (5)] yields the following expressions for the amplitudes of the first and second Josephson harmonics in terms of the bias parameter x:

$$p_1^I = x + \frac{x^3}{4}; \qquad p_1^Q = 0, \qquad (6a)$$

$$p_2^I = 0; \qquad p_2^Q = -\frac{x^2}{4}. \qquad (6b)$$

Extending the analysis to higher orders, we find the entire series of Josephson harmonics generated by a junction in its voltage state to be

$$\delta\varphi(t) = \sum_{k=1}^{\infty} p_{2k-1}^I \cos[(2k-1)\omega_J t] + p_{2k}^Q \sin[(2k)\omega_J t].$$

Such a series, with the phases of alternate even and odd harmonics shifted by $\pi/2$, is frequently encountered in nonlinear systems, for example driven ratchets, leading to directed spatial transport [7]. A similar drive configuration has also been explored to study directed diffusion in spatially periodic potentials, implemented by the tuning of activation energies with phase between the two harmonics [30]. In the particular case considered here, it corresponds to the phase across the junction evolving in a *time-asymmetric sawtooth* fashion.

As discussed for a general parametric system in the previous section, we can now study the nonlinear mixing properties of the RSJ under such time-asymmetric phase evolution. This is accomplished by treating the shunt resistor as a semi-infinite transmission line that serves as a channel for incoming and outgoing waves at the modulation frequency ω_m and sideband frequencies $\omega_\pm = \pm n\omega_J + \omega_m$ of interest [31]. We model the junction response to such input drives by including a perturbative radiofrequency (rf) component of the form $\delta\varphi_S(t) = \sum_{n=-N}^{+N} s^I \cos[(n\omega_J + \omega_m)t] + s^Q \sin[(n\omega_J + \omega_m)t]$ in Eq. (5) and performing a harmonic balance analysis at ω_m and $\omega_\pm$. The combination of the Josephson harmonics evaluated earlier plays the role of an effective multiharmonic pump. Figure 4(b) is a plot of the relative conversion
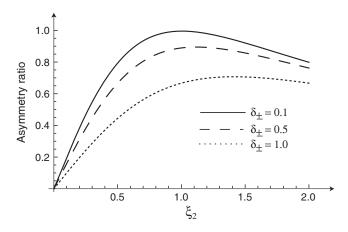
asymmetry, obtained as a difference between the net down- and up-converted amplitudes normalized to the total converted power. This asymmetry ratio is calculated by restricting the perturbative analysis to the second harmonic ($K = 2$) and the first pair of sidebands ($N = 1$) generated about the Josephson frequency [in accordance with the frequency landscape shown in Fig. 1(b)]. The figure shows that the scattering becomes nonreciprocal, with the coefficients describing down-conversion stronger than those describing up-conversion. This result is in agreement with that obtained for a general parametric mixing scheme in view of the pump configuration described by Eq. (6). Since $\alpha = +\pi/2$, the second Josephson harmonic leads the first harmonic and, as described previously, such a pump configuration leads to down-conversion (see Fig. 2). We note that the maximum asymmetry ratio obtained for the RSJ is around 0.3; this is because this ratio depends crucially on the strength of the $2\omega_J$ harmonic (Fig. 3), which in the case of RSJ is generated by a higher order process and is consequently weaker than the ω_J pump [Eq. (6)]. These results are corroborated qualitatively by those obtained through a direct numerical integration of Eq. (4) [27]. It may be possible to employ filters across the junction to modify the junction reactance near the Josephson frequency and its harmonics, and achieve a more favorable proportion of higher Josephson harmonics conducive to higher conversion asymmetry.

In conclusion, we have uncovered a generic mechanism that breaks the symmetry of frequency conversion in parametric processes. Unlike the symmetric conversion schemes employing a single frequency pump, it relies on a multiharmonic pump with appropriate relative phases and
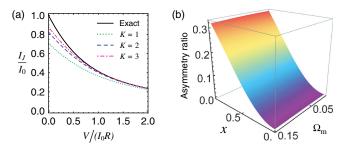

FIG. 4 (color online).   Analytical calculation for the RSJ. (a) Static $I - V$ characteristics of the RSJ calculated using the perturbative series method, showing the variation of voltage V across the junction with current I_J flowing through it. The solid black line corresponds to the exact analytical result $V = R\sqrt{I_B^2 - I_0^2}$, while the green (dotted), blue (dashed), and violet (dotted-dashed) curves correspond to the series calculation with one [$K = 1$], two [$K = 2$], and three [$K = 3$] Josephson harmonics, respectively. (b) Asymmetry ratio (cf. Fig. 3) for the RSJ, calculated with the pump configuration derived in Eq. (6). This ratio is almost independent of the modulation frequency (parametrized here as a dimensionless variable $\Omega_m = \omega_m/\omega_B$ with $\omega_B = I_B R/\varphi_0$) for small Ω_m, and increases as the junction is biased towards the strongly nonlinear regime by increasing x (or decreasing I_B) [27].

FIG. 3.   Asymmetry ratio defined as the net difference in up-converted and down-converted power, normalized to the total converted power $(|t_d|^2 + |s_d|^2 - |t_u|^2 - |s_u|^2)/(|t_d|^2 + |s_d|^2 + |t_u|^2 + |s_u|^2)$, plotted as a function of the strength of the second harmonic ξ_2, for three different detunings (or modulation frequencies). This ratio is independent of the pump strength ξ_1. The maximum ratio of unity, corresponding to 100% asymmetry, is achievable for optimal strengths of $2\omega_p$ pump and sufficiently small detunings from the carrier ($\omega_m \ll \omega_p$).

amplitudes of successive harmonics that select frequency up-conversion over down-conversion, or vice versa, with 100% efficiency. We have shown that the asymmetry in frequency conversion takes place in a current-biased RSJ. The internally generated series of Josephson harmonics has odd and even harmonics phase shifted by $\pi/2$, resulting in a pump configuration optimally tuned for down-conversion. The asymmetric frequency conversion protocol in the RSJ also provides important clues for unravelling the operation of the dc SQUID (superconducting quantum interference device) [20] as a directional, quantum-limited, microwave amplifier [18,26]. The SQUID may be modeled as a two-variable RSJ circuit with a static phase difference between the two junctions imposed by the external flux bias of the loop [26].

Given its generic platform-independent nature, our analysis opens itself to various applications. In addition to being *in situ* tunable with pump phases, the parametrically guided frequency conversion can easily be extended to a multiphoton regime without being limited by saturation effects such as those encountered in down-conversion schemes based on three-level Λ systems [32]. Selective down-conversion can also be used to enhance the generation efficiency of nonclassical states such as entangled photons [33]. Furthermore, the protocol of efficient up-conversion with gain may complement recent proposals [34] for long distance transmission of quantum information using low loss optical technology.

---

*akamal@mit.edu

[1] S. Flach, O. Yevtushenko, and Y. Zolotaryuk, Phys. Rev. Lett. **84,** 2358 (2000).

[2] M. V. Fistul, A. E. Miroshnichenko, and S. Flach, Phys. Rev. B **68,** 153107 (2003).

[3] A. V. Ustinov, C. Coqui, A. Kemp, Y. Zolotaryuk, and M. Salerno, Phys. Rev. Lett. **93,** 087001 (2004).

[4] P. Hänggi, F. Marchesoni, and F. Nori, Ann. Phys. (Berlin) **14,** 51 (2005).

[5] V. A. Shklovskij and O. V. Dobrovolskiy, Phys. Rev. B **84,** 054515 (2011).

[6] T. Salger, S. Kling, T. Hecking, C. Geckeler, L. Morales-Molina, and M. Weitz, Science **326,** 1241 (2009).

[7] P. Hänggi and F. Marchesoni, Rev. Mod. Phys. **81,** 387 (2009).

[8] B. Abdo, A. Kamal, and M. Devoret, Phys. Rev. B **87,** 014508 (2013).

[9] W. H. Louisell, *Coupled Mode and Parametric Electronics* (Wiley, New York, 1960).

[10] A. Kamal, J. Clarke, and M. H. Devoret, Nat. Phys. **7,** 311 (2011).

[11] B. Yurke, in *Quantum Squeezing*, edited by P. Drummond and Z. Ficek (Springer, New York, 2004), pp. 53–95.

[12] D. J. Kaup, A. Reiman, and A. Bers, Rev. Mod. Phys. **51,** 275 (1979).

[13] The mixing between sidebands here is a second-order, four-wave mixing process, as indicated by the exponent of the drive term entering the coefficients $v_{\pm\mp}$.

[14] P. Drummond, K. McNeil, and D. Walls, Optica Acta: Int. J. Opt. **27,** 321 (1980).

[15] P. Drummond, K. McNeil, and D. Walls, Optica Acta: Int. J. Opt. **28,** 211 (1981).

[16] A. Metelmann and A. A. Clerk, Phys. Rev. Lett. **112,** 133904 (2014).

[17] A. Metelmann and A. Kamal (to be published).

[18] L. Ranzani and J. Aumentado, arXiv:1406.4922.

[19] G.-L. Ingold, H. Grabert, and U. Eberhardt, Phys. Rev. B **50,** 395 (1994).

[20] J. Clarke and A. I. Braginski, *The SQUID Handbook Vol. I: Fundamentals and Technology of SQUIDs and SQUID Systems* (Wiley-VCH, Weinheim, 2004), and references therein.

[21] R. H. Koch, D. J. Van Harlingen, and J. Clarke, Phys. Rev. Lett. **47,** 1216 (1981).

[22] P. Joyez, D. Vion, M. Götz, M. H. Devoret, and D. Esteve, J. Supercond. **12,** 757 (1999).

[23] M. Beck, E. Goldobin, M. Neuhaus, M. Siegel, R. Kleiner, and D. Koelle, Phys. Rev. Lett. **95,** 090603 (2005).

[24] A. O. Sboychakov, S. Savel'ev, A. L. Rakhmanov, and F. Nori, Phys. Rev. Lett. **104,** 190602 (2010).

[25] K. K. Likharev and V. K. Semenov, JETP Lett. **15,** 442 (1972).

[26] A. Kamal, J. Clarke, and M. H. Devoret, Phys. Rev. B **86,** 144510 (2012).

[27] See Supplemental Material at http://link.aps.org/supplemental/10.1103/PhysRevLett.113.247003, which includes Refs. [28,29], for details of RSJ calculation.

[28] D. M. Pozar, *Microwave Engineering*, 3rd ed. (John Wiley & Sons, New York, 2005), pp. 161–182.

[29] A. A. Clerk, M. H. Devoret, S. M. Girvin, F. Marquardt, and R. J. Schoelkopf, Rev. Mod. Phys. **82,** 1155 (2010).

[30] M. I. Dykman, H. Rabitz, V. N. Smelyanskiy, and B. E. Vugmeister, Phys. Rev. Lett. **79,** 1178 (1997).

[31] Unlike the parametric model considered earlier, in the transmission line model for the RSJ we can assume that both the signal and sideband waves travel on the same spatial port as there is no resonant structure in this model. This distinction is not crucial to the problem at hand as the form of the scattering coefficients is not affected by this change, up to a common complex factor, preserving the relative phases between them.

[32] K. Koshino, K. Inomata, T. Yamamoto, and Y. Nakamura, New J. Phys. **15,** 115010 (2013).

[33] P. G. Kwiat, K. Mattle, H. Weinfurter, A. Zeilinger, A. V. Sergienko, and Y. Shih, Phys. Rev. Lett. **75,** 4337 (1995).

[34] T. Bagci, A. Simonsen, S. Schmid, L. G. Villanueva, E. Zeuthen, J. Appel, J. M. Taylor, A. Sorensen, K. Usami, A. Schliesser *et al.*, Nature (London) **507,** 81 (2014).